Journal of the Neurological Sciences 407 (2019) 116525

Contents lists available at ScienceDirect

Journal of the Neurological Sciences

journal homepage: www.elsevier.com/locate/jns

Quantifying iron deposition in the cerebellar subtype of multiple system atrophy and spinocerebellar ataxia type 6 by quantitative susceptibility mapping

Atsuhiko Sugiyama[a,b], Noriko Sato[c,*], Yukio Kimura[c], Hiroyuki Fujii[c], Norihide Maikusa[b], Yoko Shigemoto[b,c], Fumio Suzuki[c], Emiko Morimoto[c], Kyosuke Koide[a], Yuji Takahashi[d], Hiroshi Matsuda[b], Satoshi Kuwabara[a]

[a] Department of Neurology, Graduate School of Medicine, Chiba University, Chiba, Japan
[b] Integrative Brain Imaging Center, National Center of Neurology and Psychiatry, Tokyo, Japan
[c] Department of Radiology, National Center of Neurology and Psychiatry, Tokyo, Japan
[d] Department of Neurology, National Center of Neurology and Psychiatry, Tokyo, Japan

ARTICLE INFO

Keywords:
QSM
MSA-C
SCA6
Dentate nucleus
Substantia nigra

ABSTRACT

We used quantitative susceptibility mapping (QSM) to assess the brain iron deposition in 28 patients with the cerebellar subtype of multiple system atrophy (MSA-C), nine patients with spinocerebellar ataxia type 6 (SCA6), and 23 healthy controls. Two reviewers independently measured the mean QSM values in brain structures including the putamen, globus pallidus, caudate nucleus, red nucleus, substantia nigra, and cerebellar dentate nucleus. A receiver operating characteristics (ROC) analysis was performed to assess the diagnostic usefulness of the QSM measurements. The QSM values in the substantia nigra were significantly higher in the MSA-C group compared to the HC group ($p = .007$). The QSM values in the cerebellar dentate nucleus were significantly higher in MSA-C than those in the SCA6 and HC groups ($p < .001$), and significantly lower in the SCA6 patients compared to the HCs ($p = .027$). The QSM values in the cerebellar dentate nucleus were correlated with disease duration in MSA-C, but inversely correlated with disease duration in SCA6. In the ROC analysis, the QSM values in the cerebellar dentate nucleus showed excellent accuracy for differentiating MSA-C from SCA6 (area under curve [AUC], 0.925), and good accuracy for differentiating MSA-C from healthy controls (AUC 0.834). QSM can identify increased susceptibility of the substantia nigra and cerebellar dentate nucleus in MSA-C patients. These results suggest that an increase in iron accumulation in the cerebellar dentate nucleus may be secondary to the neurodegeneration associated with MSA-C.

1. Introduction

Multiple system atrophy (MSA) is a progressive neurodegenerative disease histologically characterized by the widespread presence of α-synuclein-positive glial cytoplasmic inclusions. Based on their predominant motor presentation, patients are categorized as having the MSA-Parkinson variant (MSA-P) or the MSA-cerebellar variant (MSA-C). Whether dysregulation of brain iron homeostasis acts as a primary cause of neurodegeneration or is a secondary result of cellular death in MSA remains to be elucidated. It has been suggested that dysregulation of brain iron homeostasis is related to the pathophysiology of MSA *via* oxidative stress and neuroinflammation [1], and iron deposition in the putamen has been reported as a hallmark of the disease in histopathological studies [2]. Several postmortem analyses revealed that in addition to the putamen, increased iron content was present in the substantia nigra, globus pallidus, and caudate nucleus [3,4]. Diffuse ferritin deposition in the dentate nucleus was also reported in a postmortem evaluation of patients with MSA [5].

Quantitative susceptibility mapping (QSM) was recently introduced for the quantification of brain iron distribution *in vivo* [6]. QSM is a novel post-processing technique that allows quantitative maps of the distribution of magnetic susceptibility to be calculated on the basis of gradient echo data [7]. A study investigating differences in brain iron accumulations using QSM in parkinsonian disorders (including 11 MSA patients) showed that the magnetic susceptibility values of the putamen were higher in MSA than in Parkinson's disease (PD) and healthy

* Corresponding author at: Department of Radiology, National Center of Neurology and Psychiatry, 4-1-1 Ogawa-Higashi, Kodaira, Tokyo 187-0031, Japan.
E-mail address: snoriko@ncnp.go.jp (N. Sato).

https://doi.org/10.1016/j.jns.2019.116525
Received 30 July 2019; Received in revised form 14 September 2019; Accepted 6 October 2019
Available online 13 October 2019
0022-510X/

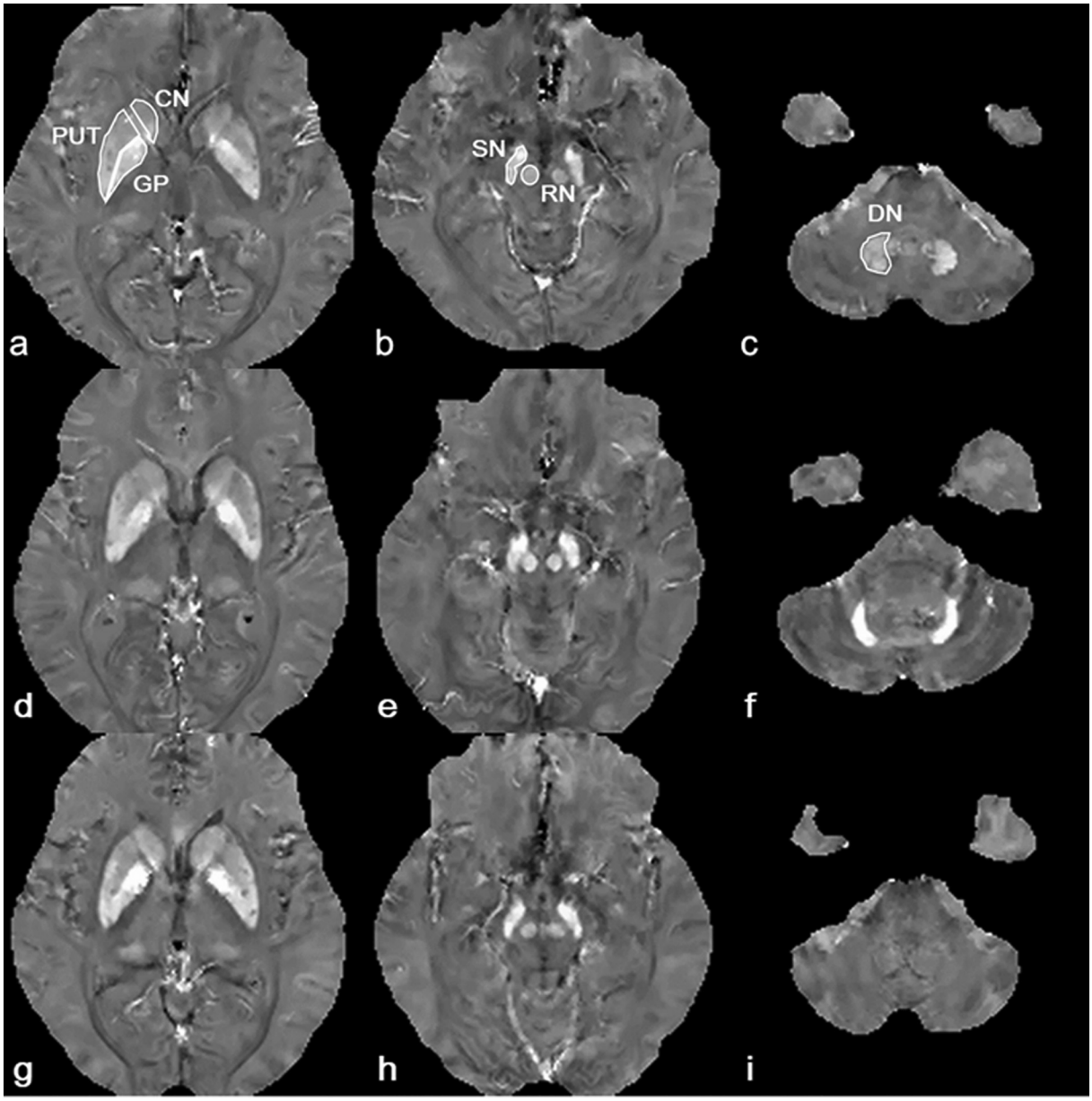

Fig. 1. Regions of interest on the QSM images and representative QSM images in MSA-C and SCA6.
ROIs drawn on the QSM map for a 65-year-old healthy male (a–c). Representative QSM images in a 66-year-old male MSA-C patient (d-f) and in a 63-year-old female SCA6 patient (g–i). DN: dentate nucleus, GP: globus pallidus, PUT: putamen, RN: red nucleus, SN: substantia nigra. (For interpretation of the references to colour in this figure legend, the reader is referred to the web version of this article.)

controls [8]. Another study using QSM in parkinsonian disorders (including six patients with MSA-P and seven patients with MSA-C) also showed that the magnetic susceptibility values of the putamen were higher in MSA-P than in PD [9]. However, sufficient *in vivo* evaluations of iron accumulation using QSM have not been performed in brain regions other than the basal ganglia in MSA—especially in MSA-C.

Spinocerebellar ataxia type 6 (SCA6) is one of the most common subtypes of autosomal dominant cerebellar ataxia [10]. Although mild pyramidal and extrapyramidal signs, sensory disturbances, and dysphagia occur in some SCA6 patients, SCA6 has been described largely as a pure cerebellar ataxia and is characterized neuropathologically by a predominant involvement of the cerebellar Purkinje cells [10,11]. In contrast to MSA, the absence of hypointensities of the iron signal on susceptibility-weighted images (SWI) in the cerebellar dentate nucleus has been observed in SCA6 patients [12]. However, quantitative evaluation of iron accumulation using QSM has not been performed in SCA6 patients. Additionally, to our knowledge, no study comparing iron accumulation between MSA-C and SCA6 using QSM has been conducted.

In the present study, we aimed to compare the iron deposition in the brains of patients with MSA-C, patients with SCA6, and healthy controls using QSM. We also investigated whether QSM can distinguish between MSA-C and SCA6. We hypothesized that the distribution and degree of iron deposition in subcortical structures are related to the underlying pathophysiology of the two disorders and would vary among the three groups. Correlation analyses were performed to evaluate the relationship between iron accumulation and selected clinical parameters, including disease duration and clinical severity, and explore whether quantifying the iron deposition using QSM may be a candidate imaging marker of disease progression.

2. Subjects and methods

2.1. Subjects

This retrospective study was approved by the institutional review board at Japan's National Center of Neurology and Psychiatry Hospital, and the need for informed consent was waved. In total, 36 consecutive MSA-C patients and 10 consecutive SCA6 patients who underwent brain MRI including the 3D multi-echo spoiled gradient echo (GRE) sequence (which is necessary for obtaining QSM) at our institution between August 2017 and January 2019 were identified in our database. Five patients with MSA-C were excluded because of poor-quality scans due to artifacts and three patients were excluded because of central nervous system involvement from another etiology (one with bipolar disorder, one with a brain infarction, and the other with a subdural hematoma). A patient with SCA6 was excluded because of poor-quality scans due to artifacts. The final groups were 28 MSA-C patients and nine SCA6 patients. Twenty-three age- and sex- matched healthy controls were also assessed by QSM.

The patients' MSA was diagnosed clinically according to the second consensus statement by Gilman et al. (probable 17, possible 11) [13]. Regarding the MSA subtypes, patients with cerebellar manifestation as initial motor symptoms and clinical syndrome dominated by cerebellar ataxia at the time of the MRI scan were classified as having MSA-C. The diagnoses of the nine SCA6 patients was genetically confirmed. The medical records of the MSA-C and SCA6 patients were reviewed, and information of their ages, disease duration, presence or absence of parkinsonism, autonomic symptoms, and Scale for the Assessment and Rating of Ataxia (SARA) scores at the time of taking the MRI were collected.

2.2. MRI studies

All MRI studies were performed on a 3-T MRI system (Philips Medical Systems, Best, The Netherlands). QSM was obtained with a 3D multi-echo spoiled GRE sequence. The imaging parameters included the following: the parameters were TE 6.5/12.9/19.3/25.7/32.1/3.5/44.9 ms; FOV 24 cm; matrix 240 × 256; flip angle 20°; voxel size 1.0 × 1.0 × 2.0 mm^3; scan time 5 min and 11 s. The QSM images were reconstructed from the complex data obtained during the GRE sequence using the morphology-enabled dipole inversion (MEDI) sequence [7].

2.3. Image analysis

Two reviewers who were blinded to the subjects' clinical data manually traced regions of interest (ROIs) using the Image J software program (U.S. National Institutes of Health, Bethesda, MD). The ROIs in the nuclei were drawn bilaterally on the basis of the anatomical structures on the QSM images, with reference to the patients' conventional MR images. The ROIs included the putamen, globus pallidus, head of the caudate nucleus, red nucleus, substantia nigra, and cerebellar dentate nucleus (Fig. 1). Data for each structure were obtained bilaterally from the two most representative consecutive slices. The mean QSM values were calculated for each structure by averaging the values on both sides of two consecutive slices, and the final values were the mean of the measurement obtained by the two reviewers. The two reviewers traced the ROIs once for all the subjects at the first session. To assess intra-rater reliability, the ROIs were traced again by one of the two reviewers at a second session after 8 months.

2.4. Statistical analysis

SPSS software ver. 25.0 (SPSS Japan, Tokyo) was used to perform all statistical analyses. The demographic data of the MSA patients, SCA6 patients, and healthy controls were compared using the χ^2 test for sex and the Kruskal-Wallis test for age at MRI. Differences in disease duration between the MSA-C patients and SCA6 patients was analyzed using the Mann-Whitney *U* test. For the evaluation of the differences in the QSM values among the groups for each brain region, a one-way analysis of covariance (ANCOVA) was used with age as covariate. The post-hoc test was performed by using the pairwise comparison of those values between groups with Bonferroni correction at $p = .05$. Spearman correlation analyses were used to assess the relationship between the disease durations of the MSA-C and SCA6 groups and the QSM values in the regions where significant differences of the QSM values were found compared to the healthy controls. Spearman correlation analyses were used to evaluate the relationship between the SARA scores of the MSA-C group and the QSM values in the regions where significant differences of the QSM values were found compared with the values recorded in heathy controls. *P*-values < .05 were considered significant.

For the assessment of the diagnostic usefulness of the QSM values, a receiver operating characteristics (ROC) analysis was performed by using the QSM values obtained from the ROIs where differences in QSM values between the groups were identified. An area under the curve (AUC) value of > 0.9 is considered excellent; an AUC value > 0.8 is considered good. The intraclass correlation coefficient was calculated for each ROI to assess the inter-rater variability with respect to the QSM values recorded by the two reviewers. The intraclass correlation coefficient was calculated for each ROI to assess the inter- and intra-rater variability in relation to the QSM values.

3. Results

The patients' and controls' demographics are summarized in Table 1. The disease duration was significantly longer in the SCA6 group compared to the MSA-C group. Of the 28 MSA-C patients, 14 had parkinsonism in addition to cerebellar ataxia at the time of taking the MRI whereas only 2 presented with isolated cerebellar ataxia without autonomic symptoms at the time of taking the MRI. Details of the clinical characteristics of the MSA-C and SCA6 patients at the time of taking the MRI are listed in Supplementary Table 1.

High intraclass correlation coefficient values were obtained (demonstrating good agreement for inter-rater measurements) in the putamen, globus pallidus, head of the caudate nucleus, red nucleus, substantia nigra, and cerebellar dentate nucleus (0.952, 0.807, 0.965, 0.913, 0.821, and 0.919, respectively; all $p < .001$). The high intraclass correlation coefficient values were good indicators for the intra-rater measurements in the putamen, globus pallidus, head of the caudate nucleus, red nucleus, substantia nigra, and cerebellar dentate nucleus (0.979, 0.984, 0.975, 0.985, 0.936, and 0.987, respectively; all $p < .001$).

The comparison of group differences of the QSM values among the MSA-C, SCA6, and HCs revealed that the QSM values in the substantia nigra were significantly higher in the MSA-C patients than in the HCs ($p = .007$, Fig. 2). The QSM values in the cerebellar dentate nucleus were significantly higher in the MSA-C patients than in both the SCA6 patients and HCs ($p < .001$, Fig. 2), and they were significantly higher in the HCs than in the SCA6 patients ($p = .027$, Fig. 2). The QSM values in all other brain regions measured did not differ significantly among the MSA-C, SCA6, and HC groups.

In the MSA-C patients, there was a significant correlation between disease duration and the QSM values in the cerebellar dentate nucleus ($r = 0.421$, $p = .026$) (Fig. 3), and there was no significant correlation between disease duration and the QSM values in the substantia nigra ($r = 0.341$, $p = .076$). In the SCA-6 patients, there was a significant inverse correlation between disease duration and the QSM values in the cerebellar dentate nucleus ($r = -0.783$, $p = .012$) (Fig. 3). In the 18 MSA-C patients who were evaluated based on the clinical severity of the disease condition using SARA, there was no significant correlation between SARA scores and the QSM values in the cerebellar dentate nucleus ($r = 0.277$, $p = .266$) and in the substantia nigra ($r = 0.396$, $p = .103$). Because only four of the nine SCA6 patients were evaluated

Table 1
Demographic data of the patients with the cerebellar subtype of multiple system atrophy (MSA-C), the patients with spinocerebellar ataxia type 6 (SCA6), and healthy controls (HC).

	MSA-C (n = 28)	SCA6 (n = 9)	HC (n = 23)	p-Value
Male/female	15/13	2/7	13/10	0.247
Age at MRI, mean ± SD (median)	63.8 ± 9.5 (64.5)	60.7 ± 9.1 (63.0)	62.9 ± 8.1 (66.0)	0.984
Disease duration, mean ± SD (median)	3.9 ± 2.5 (3.4)	9.7 ± 5.9 (9.2)	NA	0.002

NA, not applicable.

based on SARA scores at the time of taking the MRI, the correlation between SARA scores and QSM values could not be determined in SCA6 patients.

Fig. 4 summarizes the results of our ROC curve analysis of QSM values obtained from the substantia nigra and cerebellar dentate nucleus. The QSM values in the cerebellar dentate nucleus showed excellent accuracy for differentiating MSA-C from SCA6 (AUC 0.925) and showed good accuracy for differentiating MSA-C from the healthy controls (AUC 0.834).

4. Discussion

This study is the first to compare brain iron accumulation by using QSM among patients with MSA-C, those with SCA6, and healthy controls. Our analyses revealed that the QSM values in the substantia nigra were significantly higher in the MSA-C group compared to the HC group. The QSM values in the cerebellar dentate nucleus were significantly higher in the MSA-C patients than in the SCA6 and HC groups, and they were significantly higher in the HCs compared to the SCA6 group. The QSM values in the cerebellar dentate nucleus were significantly correlated with the duration of disease but not significantly correlated with SARA scores in MSA-C patients. However, the QSM values in the cerebellar dentate nucleus were inversely correlated with disease duration in SCA6 patients. In the ROC curve analysis, the QSM values in the cerebellar dentate nucleus showed excellent or good diagnostic performance to differentiate MSA-C from SCA6 or a healthy state.

The increase in the QSM values in the cerebellar dentate nucleus in MSA-C may be attributed predominantly to the increase in the iron concentration in the tissues of the regions associated with MSA-C [14]. It has been suggested that the dysregulation of iron homeostasis is associated with MSA-related neurodegeneration *via* oxidative stress and neuroinflammation and that impaired iron homeostasis can lead to abnormal iron redistribution [1]. In line with the results of the present study, a study comparing postmortem T2-weighted images of MSA-C patients with histological findings showed that hypointensity in the cerebellar dentate nucleus was associated with diffuse ferritin deposition [5]. Quantitative assessment of iron accumulation in the cerebellar dentate nucleus using QSM has also been reported in dentatorubral–pallidoluysian atrophy, one of the spinocerebellar degenerations, as MSA-C [15]. Another possible mechanism for the increased QSM values in the cerebellar dentate nucleus is atrophy in the cerebellar dentate nucleus, which may result in a relative increase in the iron concentration [16]. Although the volume of the cerebellar dentate nucleus was not evaluated in the present study, Fukutani et al. quantitatively assessed the cerebellar dentate nucleus in MSA-C patients. They reported atrophy of the dentate nucleus and an increased density of nerve cells [17].

Iron deposition in the cerebellar dentate nucleus in MSA-C patients may not be the primary cause of cerebellar dysfunction but a secondary byproduct of neurodegeneration. In the present study, the QSM values in the cerebellar dentate nucleus were significantly correlated with disease duration but were not correlated with the SARA scores in MSA-C patients. MSA-C is characterized by the primary degeneration of olivopontine nuclei and cerebellar Purkinje cells; however, the cerebellar dentate nucleus is not primarily affected [18,19]. In a study that examined the pathology of the cerebellar dentate nucleus in MSA-C, the number of dentate neurons and their efferent fibers were well-preserved, whereas afferent nerve fibers originating from the Purkinje cells, the inferior olive nucleus, and the basis pontis were severely lost [17]. A study evaluating the temporal pattern of iron deposition in the putamen of MSA patients by calculating the conditional probabilities of multimodal MRI changes also suggested that iron deposition in the putamen of MSA patients is likely a secondary byproduct of

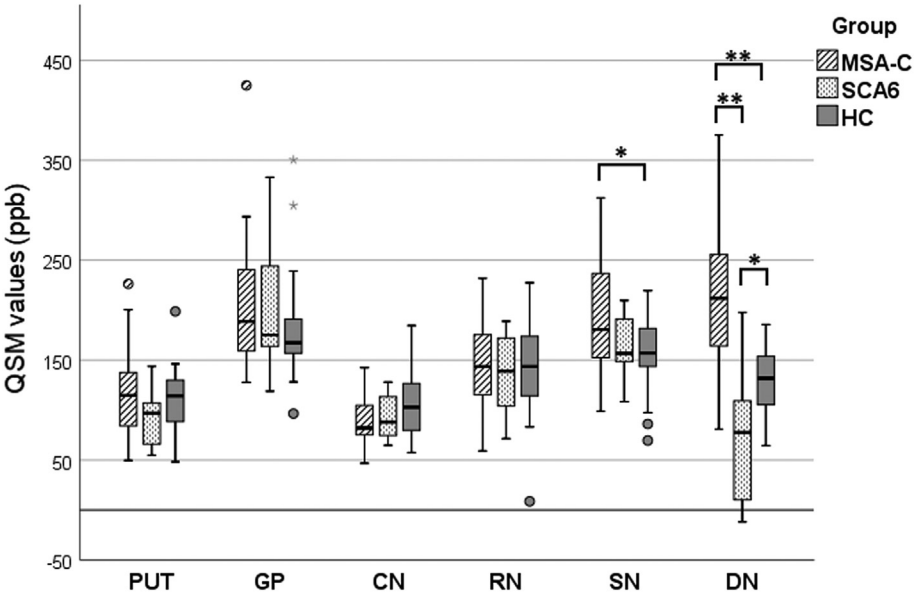

Fig. 2. Group comparisons of the QSM values in each ROI.
The units for QSM values are parts per billion (ppb). *p < .05, **p < .001. CN: head of the caudate nucleus, DN: cerebellar dentate nucleus, GP: globus pallidus, HC: HCs, MSA-C: cerebellar subtype of multiple system atrophy, PUT: putamen, RN: red nucleus, SCA6: spinocerebellar ataxia type 6, SN: substantia nigra. (For interpretation of the references to colour in this figure legend, the reader is referred to the web version of this article.)

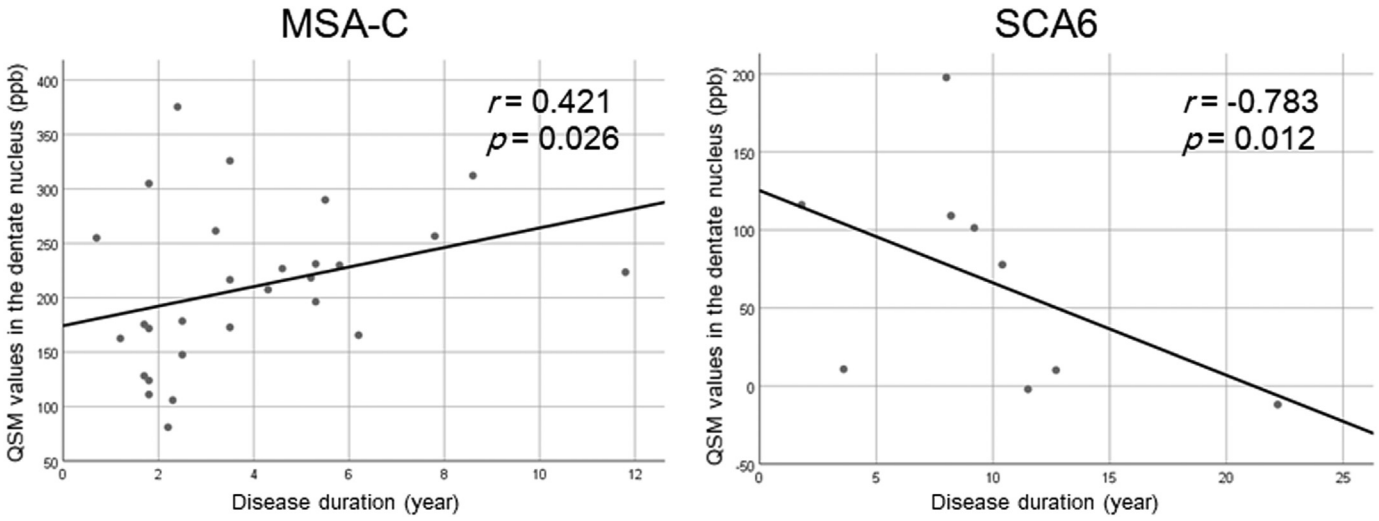

Fig. 3. Correlations between disease duration and the QSM values in the cerebellar dentate nucleus.
The QSM values in the cerebellar dentate nucleus were correlated with disease duration in MSA-C and inversely correlated with disease duration in SCA6.

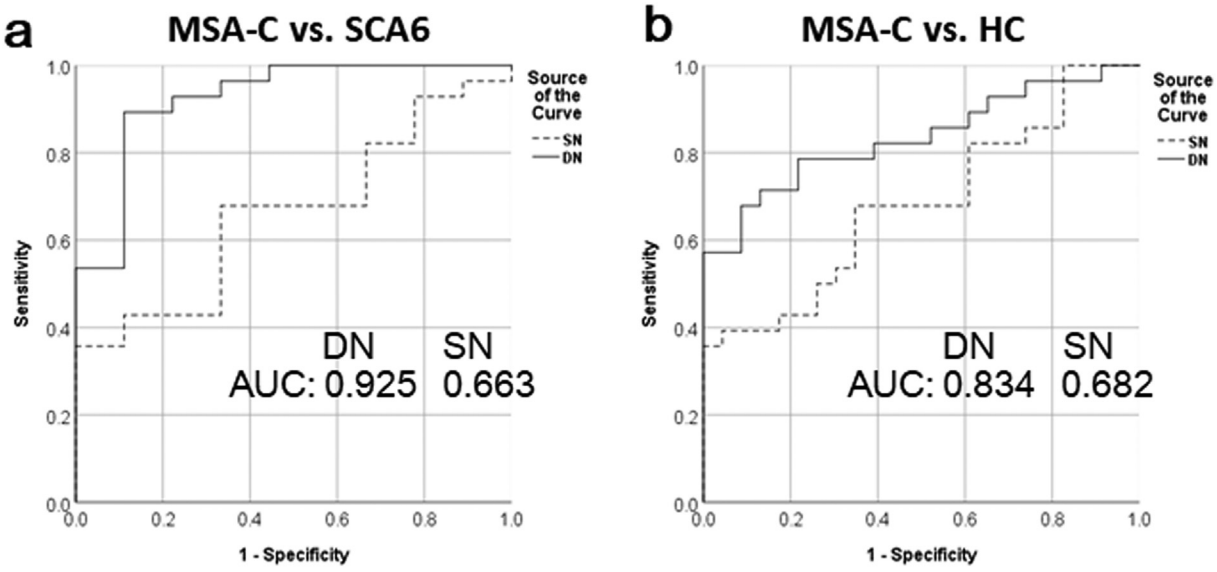

Fig. 4. ROC curve analysis of the QSM values in the substantia nigra (SN) and cerebellar dentate nucleus (DN) for diagnosis of MSA-C.
a: ROC curves showing comparisons in the SN and DN between MSA-C and SCA6. b: MSA-C and healthy controls (HC). AUC: area under the curve.

neurodegeneration [20]. To elucidate whether iron deposition in the cerebellar dentate nucleus could be an imaging marker of disease progression in MSA-C patients, a longitudinal study investigating the relationship between the amount of iron deposition in the cerebellar dentate nucleus and disease progression is required.

The QSM values in the cerebellar dentate nucleus were significantly lower in the group of SCA6 patients compared with the healthy controls and were inversely correlated with disease duration. These findings suggest a decrease in the iron content in the cerebellar dentate nucleus of SCA6 patients and that disease progression may lead to a decrease in iron deposition in the cerebellar dentate nucleus of SCA6 patients. These findings are of interest because iron deposition in the brain has been implicated in the pathogenesis of some neurodegenerative disorders and has been reported to increase with the progression of neurodegenerative disease or aging [1,21–24]. Unfortunately, we did not compare the findings of QSM images with the patients' histopathological findings; as such, the pathological background of decreased QSM values in the cerebellar dentate nucleus of SCA6 patients could not be confirmed. A possible explanation for the decreased iron content in the cerebellar dentate nucleus is the relative increase of astrocytes in the cerebellar dentate nucleus of SCA6 patients. Astrogliosis with and without neuronal loss has been reported as the pathological changes observed in the cerebellar dentate nucleus of SCA6 patients [11,25–27]. Among brain cells, the highest levels of iron content are detected in oligodendrocytes, followed by microglia and neurons, whereas the lowest iron level is found in astrocytes [28]. In line with the results of the present study, a study that evaluated the atrophy of the cerebellar dentate nucleus in SCA6 reported the absence of hypointensities of the iron signal on SWI in the cerebellar dentate nucleus in two SCA6 patients with the highest SARA scores [12]. An absence of hypointensities of the iron signal on SWI was also reported in ataxia with oculomotor apraxia type 2 [29].

Increased iron accumulation in the cerebellar dentate nucleus may play a supportive role for differentiating MSA-C patients that present with isolated cerebellar ataxia from SCA6 and healthy patients. In the ROC curve analysis of our study, the QSM values in the cerebellar dentate nucleus showed an excellent diagnostic performance in differentiating MSA-C from SCA6 or a healthy state. SCA6 can usually be

differentiated from MSA-C by a positive family history and the absence of extra-cerebellar symptoms, including parkinsonism and autonomic failure. However, autosomal dominant cerebellar ataxia has been diagnosed in patients with progressive ataxia without an apparent family history [30–32]. Moreover, patients with MSA-C often exhibit isolated cerebellar ataxia in the early course of the disease [33]. Therefore, in isolated cerebellar ataxia cases without an apparent family history, it may be difficult to distinguish between MSA-C and hereditary pure cerebellar ataxia, including SCA6. Although quantifying the iron accumulation in the cerebellar dentate nucleus using QSM may be useful in differentiating MSA-C from SCA6 in such situations, the subjects in our study included only two MSA-C patients who presented with isolated cerebellar ataxia without parkinsonism and/or autonomic symptoms. The present study did not determine whether there was a difference in the diagnostic performance between the qualitative assessment of the characteristic features on conventional MRI in MSA-C patients, such as the "hot cross bun" sign and changes in the middle cerebellar peduncle, and the quantity of iron accumulation in the cerebellar dentate nucleus using QSM for differentiating MSA-C from SCA6. Therefore, additional studies that compare QSM values in the cerebellar dentate nucleus between MSA-C patients who present with isolated cerebellar ataxia and SCA6 are needed. In addition, a comparison of the diagnostic performance between the QSM values and the qualitative evaluation of the findings on conventional MRI is also essential to better assess the clinical value of quantifying iron accumulation in the cerebellar dentate nucleus using QSM for differentiating MSA-C from SCA6.

Increased iron content in the substantia nigra has been reported in histopathological studies of MSA [3,4]. In line with these studies, we observed herein that the QSM values in the substantia nigra were significantly higher in the MSA-C group compared to the healthy controls. Although the major pathological changes in MSA-C occur in the olivopontocerebellar system rather than the striatum and substantia nigra, striatonigral degeneration was also observed in MSA-C by using histological and neuroimaging approaches [34,35]. Increased iron content in the putamen has also been reported in histopathological studies of MSA [3,4], but in the present study the QSM values in the putamen did not differ among the MSA-C, SCA6, and healthy control groups. Consistent with this result, another study using QSM showed that the putaminal QSM values in MSA-C did not different from those in PD, progressive supra nuclear palsy, and controls [9]. A longitudinal study assessing iron deposition by using R2* values also showed that the putaminal R2* values were not different between MSA-C and PD groups, whereas the putaminal R2* values were increased in MSA-P compared to those in PD at the baseline [36]. In another study that measured the putaminal R2* values in MSA, the putaminal R2* values were not different between the MSA-C patients and the control group, although the putaminal R2* values were increased in the MSA-P patients compared with those in the control group [20]. Because putaminal iron deposition in MSA tends to localize to the posterior region of the putamen with severe atrophy [37], the difference between putaminal iron deposition between MSA and other conditions may be difficult to detect when the ROI is estimated on the entire putamen.

Our study has several limitations. First, we manually delineated the ROIs rather than using an automatic or semi-automatic method, and this may have caused a potential subjective bias. However, there was consistency between the intra- and inter-rater measurements in each ROI. Second, the patients with MSA-C were clinically diagnosed without postmortem verification, and the possibility of a misdiagnosis in some of them cannot be excluded. Third, the sample size of the SCA6 group was small ($n = 9$), and further studies with larger sample sizes are needed to validate our present findings.

In conclusion, the results of our analyses demonstrated that QSM can be used to identify increased susceptibility of the substantia nigra and cerebellar dentate nucleus in MSA-C patients. The results also suggest that an increase in the accumulation of iron in the cerebellar dentate nucleus may be a secondary byproduct of neurodegeneration in MSA-C.

Supplementary data to this article can be found online at https://doi.org/10.1016/j.jns.2019.116525.

Declaration of Competing Interest

The authors declare that they have no conflict of interest.

Acknowledgements

The authors would like to thank Dr. Pascal Spincemaille and Dr. Yi Wang who provided support for introducing QSM to our facility.

References

[1] C. Kaindlstorfer, K.A. Jellinger, S. Eschlböck, N. Stefanova, G. Weiss, G.K. Wenning, The relevance of iron in the pathogenesis of multiple system atrophy: a viewpoint, J. Alzheimers Dis. 61 (2018) 1253–1273.
[2] D.W. Dickson, W. Lin, W.K. Liu, S.H. Yen, Multiple system atrophy: a sporadic synucleinoathy, Brain Pathol. 9 (1999) 721–732.
[3] D.T. Dexter, A. Carayon, F. Javoy-Agid, Y. Agid, F.R. Wells, S.E. Daniel, et al., Alterations in the levels of iron, ferritin and other trace metals in Parkinson's disease and other neurodegenerative diseases affecting the basal ganglia, Brain 114 (1991) 1953–1975.
[4] K.A. Jellinger, Neuropathological spectrum of synucleinopathies, Mov. Disord. 18 (2003) S2–S12.
[5] E. Matsusue, S. Fujii, Y. Kanasaki, T. Kaminou, E. Ohama, T. Ogawa, Cerebellar lesions in multiple system atrophy: Postmortem MR imaging-pathologic correlations, Am. J. Neuroradiol. 30 (2009) 1725–1730.
[6] B. Bilgic, A. Pfefferbaum, T. Rohlfing, E.V. Sullivan, E. Adalsteinsson, MRI estimates of brain iron concentration in normal aging using quantitative susceptibility mapping, Neuroimage 59 (2012) 2625–2635.
[7] J. Liu, T. Liu, L. de Rochefort, J. Ledoux, I. Khalidov, W. Chen, et al., Morphology enabled dipole inversion for quantitative susceptibility mapping using structural consistency between the magnitude image and the susceptibility map, Neuroimage 59 (2012) 2560–2568.
[8] H. Sjöström, T. Granberg, E. Westman, P. Svenningsson, Quantitative susceptibility mapping differentiates between parkinsonian disorders, Parkinsonism Relat. Disord. 44 (2017) 51–57.
[9] K. Ito, C. Ohtsuka, K. Yoshioka, H. Kameda, S. Yokosawa, R. Sato, et al., Differential diagnosis of parkinsonism by a combined use of diffusion kurtosis imaging and quantitative susceptibility mapping, Neuroradiology 59 (2017) 759–769.
[10] L. Schöls, P. Bauer, T. Schmidt, T. Schulte, O. Riess, Autosomal dominant cerebellar ataxias: clinical features, genetics, and pathogenesis, Lancet Neurol. 3 (2004) 291–304.
[11] K. Ishikawa, K. Watanabe, T. Yoshizawa, H. Fujita, T. Iwamoto, K. Yoshizawa, et al., Clinical, neuropathological, and molecular study in two families with spinocerebellar ataxia type 6 (SCA6), J. Neurol. Neurosurg. Psychiatry 67 (1999) 86–89.
[12] M.R. Stefanescu, M. Dohnalek, S. Maderwald, M. Thürling, M. Minnerop, A. Beck, et al., Structural and functional MRI abnormalities of cerebellar cortex and nuclei in SCA3, SCA6 and Friedreich's ataxia, Brain 138 (2015) 1182–1197.
[13] S. Gilman, G.K. Wennin, P.A. Low, D.J. Brooks, C.J. Mathias, J.Q. Trojanowski, et al., Second consensus statement on the diagnosis of multiple system atrophy, Neurology 71 (2008) 670–676.
[14] C. Langkammer, F. Schweser, N. Krebs, A. Deistung, W. Goessler, E. Scheurer, et al., Quantitative susceptibility mapping (QSM) as a means to measure brain iron? A post mortem validation study, Neuroimage 62 (2012) 1593–1599.
[15] S. Ide, S. Kakeda, H. Adachi, M. Miyata, Y. Iwanaka, K. Okada, et al., Detection of dentate nuclei abnormalities in a patient with dentatorubral-pallidoluysian atrophy using the quantitative susceptibility mapping, J. Neurol. Sci. 43 (2019) 97–98.
[16] J.H. Duyn, J. Schenck, Contributions to magnetic susceptibility of brain tissue, NMR Biomed. 30 (2017) e3546.
[17] Y. Fukutani, I. Nakamura, R. Matsubara, K. Kobayashi, K. Isaki, Pathology of the cerebellar dentate nucleus in sporadic olivopontocerebellar atrophy: a morphometric investigation, J. Neurol. Sci. 137 (1996) 103–108.
[18] A. Kume, A. Takahashi, Y. Hashizume, J. Asai, A histometrical and comparative study on Purkinje cell loss and olivary nucleus cell loss in multiple system atrophy, J. Neurol. Sci. 101 (1991) 178–186.
[19] G.K. Wenning, F. Tison, L. Elliott, N.P. Quinn, S.E. Daniel, Olivopontocerebellar pathology in multiple system atrophy, Mov. Disord. 11 (1996) 157–162.
[20] M.J. Lee, T.H. Kim, S.J. Kim, C.W. Mun, J.H. Shin, G.H. Lee, et al., Speculating the timing of iron deposition in the putamen in multiple system atrophy, Parkinsonism Relat. Disord. 63 (2019) 106–110.
[21] C.A. Habib, M. Liu, N. Bawany, J. Garbern, I. Krumbein, H.J. Mentzel, et al., Assessing abnormal iron content in the deep gray matter of patients with multiple sclerosis versus healthy controls, Am. J. Neuroradiol. 33 (2012) 252–258.
[22] E.P. Raven, P.H. Lu, T.A. Tishler, P. Heydari, G. Bartzokis, Increased iron levels and decreased tissue integrity in hippocampus of Alzheimer's disease detected in vivo with magnetic resonance imaging, J. Alzheimers Dis. 37 (2013) 127–136.
[23] S.A. Schneider, K.P. Bhatia, Excess iron harms the brain: the syndromes of

neurodegeneration with brain iron accumulation (NBIA), J. Neural Transm. 120 (2013) 695–703.
[24] P.G.D. Ward, I.H. Harding, T.G. Close, L.A. Corben, M.B. Delatycki, E. Storey, et al., Longitudinal evaluation of iron concentration and atrophy in the dentate nuclei in friedreich ataxia, Mov. Disord. 34 (2013) 335–343.
[25] C.M. Gomez, R.M. Thompson, J.T. Gammack, S.L. Perlman, W.B. Dobyns, C.L. Truwit, et al., Spinocerebellar ataxia type 6: gaze-evoked and vertical nystagmus, Purkinje cell degeneration, and variable age of onset, Ann. Neurol. 42 (1997) 933–950.
[26] K. Gierga, H.J. Schelhaas, E.R. Brunt, K. Seidel, W. Scherzed, R. Egensperger, et al., Spinocerebellar ataxia type 6 (SCA6): Neurodegeneration goes beyond the known brain predilection sites, Neuropathol. Appl. Neurobiol. 35 (2009) 515–527.
[27] X. Wang, H. Wang, Y. Xia, H. Jiang, L. Shen, S. Wang, et al., A neuropathological study at autopsy of early onset spinocerebellar ataxia 6, J. Clin. Neurosci. 17 (2010) 751–755.
[28] J.R. Connor, S.L. Menzies, S.M. St Martin, E.J. Mufson, Cellular distribution of transferrin, ferritin, and iron in normal and aged human brains, J. Neurosci. Res. 27 (1990) 595–611.
[29] S. Frismand, H. Salem, M. Panouilleres, D. Pélisson, S. Jacobs, A. Vighetto, et al., MRI findings in AOA2: cerebellar atrophy and abnormal iron detection in dentate nucleus, Neuroimage Clin. 2 (2013) 542–548.
[30] L. Schöls, S. Szymanski, S. Peters, H. Przuntek, J.T. Epplen, C. Hardt, et al., Genetic background of apparently idiopathic sporadic cerebellar ataxia, Hum. Genet. 107 (2000) 132–137.
[31] M. Abele, K. Bürk, L. Schöls, S. Schwartz, I. Besenthal, J. Dichgans, et al., The aetiology of sporadic adult-onset ataxia, Brain 125 (2002) 961–968.
[32] M. Hadjivassiliou, J. Martindale, P. Shanmugarajah, R.A. Grünewald, P.G. Sarrigiannis, N. Beauchamp, et al., Causes of progressive cerebellar ataxia: prospective evaluation of 1500 patients, J. Neurol. Neurosurg. Psychiatry 88 (2017) 301–309.
[33] S. Gilman, R. Little, J. Johanns, M. Heumann, K.J. Kluin, L. Junck, et al., Evolution of sporadic olivopontocerebellar atrophy into multiple system atrophy, Neurology 55 (2000) 527–532.
[34] K.A. Jellinger, K. Seppo, G.K. Wenning, Grading of neuropathology in multiple system atrophy: proposal for a novel scale, Mov. Disord. 20 (Suppl. 12) (2005) S29–S36.
[35] E. Muñoz, A. Iranzo, S. Rauek, F. Lomeña, J. Gallego, D. Ros, et al., Subclinical nigrostriatal dopaminergic denervation in the cerebellar subtype of multiple system atrophy (MSA-C), J. Neurol. 258 (2011) 2248–2253.
[36] J.H. Lee, T.H. Kim, C.W. Mun, T.H. Kim, Y.H. Han, Progression of subcortical atrophy and iron deposition in multiple system atrophy: a comparison between clinical subtypes, J. Neurol. 262 (2015) 1876–1882.
[37] E. Matsusue, S. Fujii, Y. Kanasaki, S. Sugihara, H. Miyata, E. Ohama, et al., Putaminal lesion in multiple system atrophy: postmortem MR-pathological correlations, Neuroradiology 50 (2008) 559–567.